Relative quiescence in the stress-shadow regions prior to the large earthquakes off the east coast of Miyagi Prefecture, northern Japan, and its implication for the intermediate-term prediction

Yosihiko Ogata

Institute of Statistical Mathematics, Tokyo. Email; ogata@ism.ac.jp

Abstract.

This paper is concerned with the intermediate-term prediction of the forthcoming M7 ~ 8 class earthquake on the plate boundary, off the east coast of Miyagi Prefecture, northern Japan, which is the highest probability among the long-term forecast announced to the public. Regional seismicity in the regions of stress-shadow preceding each of the previous ruptures in 1936 and 1978 shows quiescence relative to the predicted rate by the ETAS model (the relative quiescence), whereas the seismicity is well predicted in the regions of neutral or increasing Coulomb failure stress (CFS), which leads to the effect of possible precursory slip within or near the source. Anticipating similar scenarios, a number of sequences of earthquakes or aftershocks from the activities during 1979-2004 in northern Japan are analyzed by fitting the ETAS model to examine the relation to the CFS increments in the considered regions using the source model of the 1793, 1936 and 1978 ruptures. Surmising the precursory slips, it is likely that the results of the normal activity and relative quiescence in respective activities are due to those of the 2003 Miyagi-Ken-Oki intra-slub earthquake of M7.0 rather than those of the expected rupture on the plate boundary. Thus, it is unlikely that the predicted rupture will imminently occur within a couple of years from the analyzed time of 2004, but it is recommended to monitor the future activity to detect the anticipated relative quiescence in the stress shadow areas due to the interplate rupture models.

Key words; Aftershock sequences, Coulomb failure stress, ETAS model, Seismicity rate change, Precursory slips

1. Introduction.

Precursory seismic quiescence as a predictor of large earthquakes has attracted much attention amongst seismologists in the last several decades ever since Inouye (1965) first proposed the concept. Utsu (1968), Ohtake et al. (1977), Wyss and Burford (1987) and Kisslinger (1988) have successfully predicted subsequence large earthquakes in the past, although many other papers regarding the precursory seismic quiescence have been retrospective (postdiction). This suggests that we need much more research into the relation between the quiescence and subsequent earthquake activity for an effective prediction. We should also explain how quiescence can take place in a much wider area than the rupture source (e.g., Inouye, 1965 and Ogata, 1992).

On the other hand, the concept that the stress changes due to a slip can be the mechanism by which another event is triggered (Reasenberg and Simpson, 1992; King et al., 1994; Stein, 1999; Toda et al., 2002) has also received much attention of late. Additionally, seismic quiescence due to coseismic stress-lowering transferred from a rupture (stress shadow, e.g., Harris, 1998; Toda and Stein, 2002) has been discussed as a general phenomenon. Typically, quiescence is visible in regions where activity has been high, while activation is visible in regions where activity has been low.

Ogata (2004a, b, c, d and 2005) discusses the precursory quiescence relative to the modeled rate (the relative quiescence) in the stress shadow regions owing to the possible silent slips in and around asperities (e.g., Yamanaka and Kikuchi, 2004; Uchida et al., 2003, 2004) in the focal rupture. However, given relative quiescence, the difficulty is to identify the location and meaning of slips; that is, how close the slip is to the major asperity and how imminent it is to the main rupture. Further, it may be in an area of the habitual slipping only. Thus, in order to make a probability forecast of a large earthquake, we need to make and examine possible scenarios based on the available knowledge in seismology, tectonics etc.

The Headquarters for Earthquake Research Promotion of Japan (2005) recently announced a high probability for the long term forecast (about 50%, 90% and 99% within 10, 20 and 30 years, respectively, at the time instance of January 2005) of a strong interplate earthquake of M7 ~ 8 class on the plate boundary off the coast of Miyagi Prefecture (Miyagi-Ken-Oki), northern Japan, which was predicted based on a recompiled historical data of the earthquakes of 1793 (M8.2), 1835 (M7.3), 1861 (M7.4), 1897 (M7.4), 1936 (M7.4), and 1978 (M7.4). Here the 1793 event of M8.2 has an

extraordinarily wider rupture area than the others. This is based on a recalculation of Utsu (1984), by fitting renewal process models to the data of the region compiled by Seno (1979).

In 28 May 2003, the M7.1 earthquake at Miyagi-Ken-Oki (Miyagi Prefecture offshore) took place within the Pacific Plate subducting beneath the Tohoku District (North American Plate), an event that was followed by a destructive inland earthquake of M6.2 (e.g., Ogata, 2005). These made people more concerned about the occurrence of the predicted interplate strong earthquake.

This paper is concerned with some seismic features inland and in the vicinity of the Tohoku District, northern Japan (cf. Figure 1 and others) prior to the interplate earthquakes, which may be useful for the intermediate term prediction of such earthquakes. Specifically, I first study the earthquake sequences from the neighboring offshore areas, Tohoku District inland and the western offshore region in the Sea of Japan prior to the last two Miyagi-Ken-Oki earthquakes in November 1936 (M7.4) and in June 1978 (M7.4). These features are then compared with recent seismic activities from various regions. This paper assumes that significant intermittent slips occur within and near the source of the respective earthquake due to the acceleration of quasi-static (slow) slips on the plate boundary as the time of rupture of the major asperity approaches, which is indicated by the analysis of small repeating earthquake data (Uchida et al., 2003, 2004). Thus, this paper looks carefully at the seismicity in the stress-shadow transferred from the slip, including aftershocks of other large earthquakes. Such a scenario for intermediate earthquake prediction is expected to be useful for explaining the features of data set from the current seismicity.

2. Method

In order to recognize slight systematic seismicity changes, we need to fit a suitable statistical model to the normal seismic activity, prior to the suspected anomaly time. Consider the ETAS model (described in the Appendix) representing the occurrence rate of earthquakes $\lambda_\theta(t)$ at time t in a well-defined seismic region; the occurrence rate is formally the differential of occurrence probability of an event, and is dependent not only on the elapsed time t but also on the occurrence times and magnitudes of previous events. The characterizing parameter θ and the occurrence history do not depend on the location of earthquakes. Given a dataset of the occurrence times associated with corresponding magnitudes, we can obtain estimates of the parameters of the model as shown in the Appendix.

We can then see clearly the goodness-of-fit of the estimated model to an earthquake sequence by comparing the cumulative number of earthquakes against elapsed time with the predicted number. Suppose that a series of events $\{ t_0, t_1, ..., t_N \}$ are generated by a statistical model $\lambda(t)$, which is the predicted occurrence rate of events per unit time (i.e., day). Then consider the integral

$$\Lambda(s,t) = \int_s^t \lambda(\sigma)\, d\sigma \qquad (1)$$

which is the theoretical cumulative number of the events in the time interval (*s, t*) to be compared with the actual number of earthquakes *N*(*s, t*) in the same interval. For example, $\Lambda(S,t) = K\{\ln(t+c) - \ln(S+c)\}$ in the case of the original Omori model $\lambda(t) = K(t+c)^{-1}$. See Ogata and Shimazaki (1984), Matsu'ura (1986), Ogata (1988, 1992, 1999), Utsu et al. (1995) for further examples. If we consider the time change $\tau_i = \Lambda(S, t_i)$ from t to τ, then $\{ t_1, t_2, ..., t_N \}$ is transformed one-to-one to $\{ \tau_1, \tau_2, ..., \tau_N \}$, which distribute uniformly random in the interval [*0, Λ*(*S, T*)].

Therefore, if the seismicity rate $\lambda_{\hat{\theta}}(t)$ estimated from the events in the interval [*S, T*] is a good approximation to the real seismicity, then we can expect not only that the function curve $\Lambda(S, t)$ of time *t* and the empirical cumulative function N(*S, t*) of events are fairly overlapping to each other until time *T,* but also that the extrapolated cumulative function $\Lambda(S, t)$ of $t \geq T$ offers a good prediction of the actual cumulative number of earthquakes in the period after time *T*. Similarly, the transformed data $\{ \hat{\tau}_1, \hat{\tau}_2, ..., \hat{\tau}_{N+M} \}$ from the real occurrence data are uniformly distributed on the interval $[\,0, \Lambda(S,t)\,]$ where *N* = N(*S, T*) and *M* = N(*T, t*) if and only if the model is correct; namely, we see that the cumulative number (i.e., *i*) becomes a linear function of the transformed time $\tau_i = \hat{\Lambda}_{\hat{\theta}}(S, t_i)$.

Our concern is then with the significant activation and lowering of the seismicity relative to that predicted by the model, from which we explore the relationship to the change pattern of the Coulomb failure stress (*CFS*) transferred from a rupture or silent slip elsewhere. Changes in seismic activity rate are often reported to correlate with the calculated Coulomb failure stress change

$$\Delta CFS = \Delta(\textit{shear stress}) - \mu\,\Delta(\textit{normal stress}) \qquad (4)$$

(e.g., Reasenberg and Simpson, 1992; Toda and Stein, 2002), where μ represents the apparent friction coefficient, and positive normal stress means the compression. Throughout this paper we

set μ = 0.4, so as to minimize the uncertainty of ΔCFS in μ as discussed by King et al. (1994), with the results of ΔCFS patterns generally being stable against their perturbation, unless receiver faults are close to the ruptured fault. The Coulomb stress change in an elastic half-space (Okada, 1992) is calculated by assuming a shear modulus $3.2\times10^{11} dyn\ cm^{-2}$ and a Poisson ratio of 0.25. Positive values of ΔCFS promote failure and negative ones inhibit failure. The negative ΔCFS is called a stress shadow. To set the receiver fault mechanisms in Table 2 and 3, the readers are referred to Ichikawa (1971), Research group for active faults in Japan (1992), Japan Meteorological Agency (2004), Kikuchi and Yamanaka (2003), and Tohoku University (1995). Throughout this paper the size of the precursory slip is assumed to be 10% as large as the rupture, and as is the ΔCFS value of the precursory relative to the coseismic one. We then rely on the seismicity rate change based on the rate-and-state friction law (Dieterich, 1994) as the quantitative basis of the triggering (cf., Discussions of this paper).

3. Relative quiescence in the stress-shadow regions prior to the 1937 and 1978 earthquakes

The source model of the 1937 earthquake is listed in Table 1. The first available hypocenter data prior to the occurrence of this rupture is the shallow activity (depth < 35km) of earthquakes of M4.0 or larger that occurred during the period 1926-1937, in and around the Tohoku District, as shown in Figure 1. Figure 1a shows the 1937 source model and the epicenter map of shallow moderate earthquakes. Consider the earthquakes from the stress shadow regions (gray region) where the predominant mechanism is the E-W compression reverse fault type (cf., Table 2). The quiescence during the period 1935-36 prior to the main event (dotted vertical line) can be seen in the stress-shadow region, where the ΔCFS ranges - 1 ~ - 20 millibars by assuming 10% of the slip-size of the 1936 rupture. Hereafter, preslips are assumed to be 10% of the size of the main rupture.

The next earthquake sequence is taken from the seismic activity that mostly includes the aftershocks of the 1933 great Sanriku-Oki earthquake of M8.3, which caused a disastrous tsunami and which is also famous for being a normal faulting type (Kanamori, 1972) due to its proximate location to the subducting trench (Lin and Stein, 2004). The aftershock area (grey color rectangle) is mostly covered by the stress-shadow with ΔCFS value ranging - 5 ~ - 1 millibars, transferred from the assumed preslip of the 1936 Miyagi-Ken-Oki earthquake of M7.5. Here I have assumed that the majority of aftershocks and background events around this region have similar normal faulting to

the 1933 event (cf., Table 2). The ETAS model is applied to the events in the gray region of stress shadow in Figure 2a (cf., Table 2). The result shown in Figure 2b suggests that the quiescence relative to the ETAS model started around the end of 1933; that is, about three years prior to the focal rupture of 1937.

At the same time, we investigate the seismicity during the period 1926-1938 in region B in Figure 2a, where the great swarm at Shioya-Oki (Ms 7.4, 7.7, 7.7, 7.6, and 7.0) started in November 1938. Abe (1977) noted several unusual features of these shocks, such as a swarm of large earthquakes, the large energy release comparable to Ms=8.1, and the inferred fact that there had been no major earthquakes about the focal region for at least the past 800 years, whereas the ordinary recurrence time of the large earthquakes of $M \geq 7.5$ occurring in the other parts of the same plate boundary was usually less than a hundred years. The ruptures of the great swarm seem to be accelerated by the 1936 Miyagi-Ken-earthquake. Indeed, Figure 2c shows that the coseismic activation due to the 1936 rupture where ΔCFS value ranges 0.05 ~ 2 bars in the region B. However, we see that the activity up until the 1936 event is well predicted by the ETAS model, and the relative activation of the activity before the 1936 event is not seen: Readers are referred to a discussion of this paper for the reasons of the detection insensivity of the relative activation compared to the relative quiescence.

The last interplate rupture of M7.4 in this region occurred on June 12, 1978, the source model of which is also listed in Table 1. Figure 3a shows the epicenter map of moderate earthquakes that occurred from 1964 through 1980, including the aftershocks of the 1964 Niigata earthquake of M7.5. Figure 3a also shows the considered stress shadow regions (gray region) where E-W compression reverse fault type mechanisms are predominant. Then, Figure 3b indicates that the relative quiescence lasted about 7 years from 1970 up until the time of the rupture (vertical dotted line).

On the other hand, the seismicity ($M \geq 5.0$) including the aftershocks of the 1968 great Tokachi-Oki earthquake of M7.9 shown in Figure 4a is the region of the neutral or very slight *CFS* increase (cf., Table 2), assuming preslip of the 1978 Miyagi-Ken-Oki earthquake of M7.4 and also assuming that the majority of the aftershocks are of thrust type mechanisms similar to the 1968 mainshock (Table 2). In this case, we see no seismicity changes even after the 1978 rupture (Figure 4b).

About 4 months before the interplate M7.5 rupture, the Ojika-Hanto-Oki earthquake of M6.7

occurred at 20 February, 1978, within the subducting slub at (142.20E, 38.75N), the northern vicinity of the M7.5 interplate source, while this is intraplate thrust rupture within the subducting Pacific Plate (cf., Table 2). Figure 5 shows that the aftershock activity of M4 or larger is inhibited for about two months before the rupture. The aftershocks are in the stress shadow region with ΔCFS of about -100 millibars transferred from the assumed preslip which is 10% of the size of the M7.4 interplate rupture. Incidentally, such a slip could be triggered by the former mainshock, with a few bars' ΔCFS.

To summarize, the seismicity in the regions of stress-shadow shows quiescence relative to the predicted rate by the ETAS model (the relative quiescence) before each of the previous ruptures in 1936 and 1978, whereas the seismicity is well predicted in the regions of neutral or increasing Coulomb failure stress (*CFS*). Thus, the possible precursory slip within or near the source are anticipated for the scenario of predicting a forthcoming rupture.

4. Analyses of the recent seismicity and the scenarios of the precursory slips

In this section we examine whether the relative quiescence can be seen in the sequences of recent earthquakes from the stress shadow regions, assuming the occurrence of precursory slips within or in the vicinity of the interplate sources. Here I consider all the source models of the 1793, 1936 and 1978 interplate ruptures (top three rows of Table 1) in addition to the recent intra-slub rupture, i.e., the 2003 event of M7.1 at Miyagi-Ken-Oki (the bottom row of Table 1) that has a similar mechanism to that of the 1978 Ojika-Hanto-Oki earthquake (cf., Table 2). The results are then interpreted in view of the *CFS* increment.

In the first case, we consider the earthquakes that occurred during the period from 1978 to 20 July, 2003, including aftershocks of the 1984 Central Sea of Japan earthquake of M7.7, in the stress-shadow region (gray region) indicated in Figure 6a, where E-W compression reverse fault type mechanisms are predominant. Figure 6b shows that the sequence of events took place as predicted by the ETAS model. This seems to indicate no significant slips have taken place yet for a stress-shadow that could inhibit the normal aftershock activity, since a preslip of 10% of the size of the rupture models should decrease the stress with the ΔCFS ranging - 10 ~ - 1 millibars. On the other hand, if we assume the pre-slip of the 2003 May Miyagi-Ken-Oki earthquake, the region

would have an increase of the Δ*CFS* ranging +0.3 ~ +2 millibars, which may well explain the fact that we do not see any relative quiescence.

The second case considers earthquakes in the region indicated in Figure 7a, which includes the aftershocks of the 1994 Sanriku-Haruka-Oki earthquake of M7.5 and background activity in and around the region where reverse fault type mechanisms are predominant due to the plate boundary. Figure 7b shows that the sequence of events occurred as predicted by the ETAS model. Assuming that the majority of the aftershocks are of thrust type mechanisms similar to the 1994 mainshock of M7.5 (Table 2), the aftershock area (grey color rectangle) is in the stress increase with Δ*CFS* values ranging +0.5 ~ +8 millibars or +0.1 ~ +0.5 millibars, transferred from the assumed preslips of the interplate rupture models or the 2003 intra-slub rupture of M8.1, respectively.

The third case examines the aftershock sequence of the 26 May, 2003 Miyagi-Ken-Oki earthquake of M7.1 itself (cf., Table 1). This occurred within the subducting slub with a similar mechanism to the previously mentioned 1978 Ojika-Hanto-Oki earthquake (see Tables 2 for Fig. 5). In this case, we see no seismicity changes and the cumulative number of aftershocks up until now (June 2005) is very well predicted by the Omori-Utsu formula (Figure 8), unlike the case of the Ojika-Hanto-Oki earthquake (Figure 5).

Finally, the ETAS model is fitted to the aftershock sequences of the 26 July, 2003 inland shallow earthquake of M6.3 in northern Miyagi-Ken, occurring until the present (10 June 2005). From Figure 9 we see no seismicity changes and the cumulative number of aftershocks up until now (June 2005) is very well predicted by the ETAS model.

To summarize, all the analyzed results in this section are normally predicted by either the Omori-Utsu formula or the ETAS model. There may be no significant preslips to make the seismicity changes in the considered cases. However, if any preslip took place during the considered period, that of the 2003 Miyagi-Ken-Oki intra-slub earthquake of M7.1 is more likely than those of the expected ruptures on the plate boundary.

5. **Analyses of recent inland seismicity clusters, and their relation to stress-changes based on the possible scenarios of precursory slips**

In this section, the earthquake sequences from local clusters in the vicinity of the forthcoming focal interplate event are examined by fitting the ETAS to discriminate whether it is well adapted

throughout the entire period up to the present time or whether it becomes quiet relative to the modeled rate. Also, we calculate the Δ*CFS* in the region transferred from the possible precursory slips on the plate boundary (cf., top three rows of Table 1), in addition to the 2003 intraplate rupture of M7.1 (the bottom row of Table 1). The results are then interpreted in view of the *CFS* increment.

Figure 10 shows the regions A - E of the seismic clusters during the period 1995 – July 2003. The considered clusters are (A) recent aftershock activity of the 1962 Miyagi-Ken-Hokubu earthquake of M6.5, (B) swarm activities of the 1996 Miyagi-Ken Naruko-Machi earthquake of M5.9, (C) the seismicity including the aftershocks of the 1998 Miyagi-Ken-Nanbu earthquake of M5.0 that occurred in Sendai city, (D) the seismicity including the aftershocks of the 1998 Iwate-Ken-Shizukuishi earthquake of M6.1, and (E) aftershocks of the 2002 Miyagi-Ken-Oki earthquake of M6.1. The predominant angle of the receiver fault in each cluster is assumed to be similar to their mainshock mechanism (cf., Table 3).

Table 3 also lists Δ*CFS* values assuming precursory slips due to either the 2003 Miyagi-Ken-Oki intra-slub earthquake of M7.1 or the interplate rupture models in Table 1. All the results are consistent with the assumed preslip of the 2003 Miyagi-Ken-Oki earthquake of M7.1, rather than that of the forthcoming interplate rupture models.

In addition, the quiescence preceding the 2003 Miyagi-Ken-Oki earthquake of M7.1 is clearly seen in the depth versus time plot in Figure 3 of Ogata (2005) due to the precursory slip within the source, the onset of which appeared to be triggered by the 2002 event of M6.1 with about +50 millibars, and in turn the precursory slip seems to have inhibited the activity in the neighboring plate boundary region with - 20~ - 5 millibars (cf., Figure 3 in Ogata, 2005) including the aftershock activity of the M6.1 event itself (see Figure 9E). Incidentally it is less likely that the quiescence of the aftershock activity of the M6.1 event is triggered by the preslip of the forthcomming interplate rupture of the 1978 Miyagi-Ken-Oki type, because of the positive Δ*CFS* values ranging +8~+10 millibars in the same region.

To summarize, all the analyzed results in this section are consistent with the assumed preslip of the 2003 Miyagi-Ken-Oki earthquake of M7.1, contrary to the assumed preslip of the expected interplate rupture. Thus, it is likely that the results of the normal and relative quiescence are due to those of the 2003 Miyagi-Ken-Oki intra-slub earthquake of M7.0, rather than those of the expected rupture on the plate boundary.

6. Discussions

Since a sequence of aftershocks is triggered by complex mechanisms under fractal random media, it is difficult to calculate the transfer of stresses both within and near to the field. That is, triggering mechanics within an aftershock sequence are too complex to calculate the effect of stress changes. Therefore, the statistical empirical laws of aftershocks are very useful as a practical solution to the proximate triggering effect. In other words, fitting and extrapolating a suitable statistical model for normal seismic activity in a situation without exogenous stress changes provides us with an alternative method through which we can detect the seismicity changes sensitively. Thus, the diagnostic analysis based on fitting the ETAS model is helpful in detecting small exogenous stress changes. Indeed, these changes are so slight that even current state of the art methods and the geodetic records from the GPS network can barely recognize systematic anomalies in the time series of displacement records.

Few results in the present manuscript agree with the claim that there should be a threshold value of ΔCFS capable of affecting seismic changes. Although the stress change values can be very small in the order of a few millibars or less, the number of earthquakes in the receiver region is fairly large so that we have statistically significant seismicity rate change depending on the sample size, too. Thus, we expect that significant deviation of actual activity from the predicted rates is sensitive enough to detect a slight stress-change.

Compared to the relative quiescence, the relative activation is not very sensitive, because the shear-stress-increase triggered by the large aftershock surpasses the exogenously triggered effect from other sources. Therefore, its effect is hard to see in the diagnostic analysis by the ETAS model unless the *b*-value of the G-R magnitude frequency significantly increases (i.e., increase of the ratio of the smaller events to the larger events). The reason why the regional activation is not easy to detect compared to the quiescence is because of the definition of the ETAS model itself, and because many aftershocks are triggered by much higher ΔCFS values than the regional ΔCFS effect.

Also, the ratio of future to past seismicity rates (R/r) due to Dieterich (1994) for a positive Coulomb failure increment is less effective than the negative increment of the same absolute value, where

$$R(t) = \frac{r}{\left[\exp\left\{\frac{-\Delta CFF}{A\sigma_n}\right\} - 1\right]\exp\left(\frac{-t}{\dot{\tau}}\right) + 1},$$

where A is a fault constitutive parameter, σ_n is the normal stress, and $\dot{\tau}$ is the shear stressing rate. We see the slower decay of quiescence factor $R(t)/r$ with time t than that of activation, and also the reciprocal of the reduction factor $R(+0)/r$ of the seismicity lowering rate change is larger than the enhancement one of activating rate. Ogata (2004c and d) demonstrates these by assuming the appropriate parameters of the equation and this should become more conspicuous for smaller values of $A\sigma$ (where A is a fault constitutive parameter).

The empirical evidence of the R/r-curve is seen, in Reasenberg and Simpson (1992) and Toda et al. (1998) for the case of positive ΔCFS, but is not clearly seen for the negative case. This is because their data is mostly from background seismicity. The decrease of R/r is seen only when the seismicity rate r is high enough, while an increase of R/r is easily seen, whichever r is. On the other hand, the relative quiescence can be sensitively observed in a high rate aftershock activity.

Conclusions

The ETAS model is useful and indispensable for detecting slight stress changes. We have seen that the relative quiescence is revealed in the seismic activity or aftershocks from the stress-shadow area preceding each of the large 1936 and 1978 interplate recurrent ruptures in the Miyagi-Ken-Oki, whereas the seismicity in the regions of the neutral or positive ΔCFS normally undergoes changes as predicted by the ETAS model.

A number of sequences of earthquakes or aftershocks from the activities during the period 1979-2003 in northern Japan are analyzed by fitting the ETAS model to discriminate whether the sequence has relative quiescence or is normal, and further to examine the match between the normal or anomaly and the *CFS* increments in the considered regions, using the source model of the 1793, 1936 and 1978 ruptures. Surmising the precursory slips, it is likely that the results of the normal activity and relative quiescence of the recent activities in respective areas are due to those of the 2003 Miyagi-Ken-Oki intra-slub earthquake of M7.0, rather than those of the expected rupture on the plate boundary; namely, it is unlikely that the predicted rupture will occur imminently within a couple of years from the analyzed time of 2004.

However, from the long-term prediction, it is very likely that we will have the predicted interplate rupture within the next couple of decades. From the results summarized in this paper, it will be useful to continue monitoring the activity to detect the relative quiescence in the stress shadow areas, such as the wide regions in Figures 1, 2A, 3, and 6, intra-slub aftershocks like Figure 5, and inland cluster activity in Figures 9, 10A and 10B (cf., Tables 2 and 3).

Acknowledgments

I have used the TSEIS visualization program package (Tsuruoka, 1997) for the study of hypocenter data, and also used the PC program MICAP-G for spatial visualization of Coulomb stress changes (Naito and Yoshikawa, 1998). This study is partly supported by Grant-in-Aid B2-14380123 and A-17200021 for Scientific Research, Ministry of Education, Science, Sports and Culture.

Appendix: Models and model fitting

The typical aftershock decay is represented by the Omori-Utsu formula (Omori, 1894; Utsu, 1961; Ogata, 1983; Utsu et al., 1995),

$$\nu(t) = K(t + c)^{-p}, \quad (K, c, p; \text{constant}), \qquad (2)$$

initiated by the main shock at time origin $t=0$. In general, this formula holds for quite a long period in the order of some tens of years or more, depending on the background seismicity rate in the neighboring area (Utsu, 1969; Ogata and Shimazaki, 1984; Utsu et al., 1995). As we consider small aftershocks, however, occurrence-time clustering of the events within the aftershock sequence becomes apparent. Thus, aftershock activity is not best predicted by the single Omori-Utsu formula, especially when it includes conspicuous secondary aftershock activities of large aftershocks, as demonstrated in Guo and Ogata (1997) and Ogata et al. (2003). Indeed, we see cascading complex features of aftershocks, such as interactively triggered aftershocks, including off-fault aftershocks. Therefore, we assume that every aftershock can trigger its own further aftershocks or remote events greater or small in magnitudes, and that the occurrence rate at time t is given by a (weighted) superposition of the Omori-Utsu functions ν in (2) shifted in time

$$\lambda_\theta(t) = \lambda_0 + \sum_j e^{\alpha\{Mj - M_c\}} \nu(t - t_j), \qquad (3)$$

where the summation is taken over every *j* for the aftershock occurred before time *t* (days). The constant λ_0 (shocks/day) represents occurrence rate of the seismicity factor, which cannot be explained by the aftershock effect from the past events whose record is available in the data (so-called the background seismic activity). The weighted size of its aftershocks is made by the exponential function of its magnitude M_j as in (3) in accordance with the study by Utsu (1970), where M_c represents the cut-off magnitude of the fitted data in order to maintain the homogeneity of the magnitude frequency distribution throughout the studied period. The coefficient α (magnitude^{-1}) measures an efficiency of a shock in generating its aftershock activity relative to its magnitude. Note that the standardized quantity *K* (shocks/day) in the ν-function measures the productivity of the aftershocks during a short period right after the mainshock (Utsu, 1970; Reasenberg and Jones, 1989). We call the equation (3) the epidemic-type aftershock sequence (ETAS) model, which was originally proposed for the general seismic activity in a region (Ogata, 1988). Five parameters λ_0, *K*, *c*, **α**, and *p* represent characteristics of seismic activity of the region. If the observed rate of occurrence is compared with the calculated one from the model, period of decreased or increased seismic activity (relative quiescence or activation) can be recognized.

Then, given a sequence of occurrence times associated with magnitudes $\{ (t_i, M_i) \}$ during an observed period [*S*, *T*], the characterizing parameters θ are estimated by maximizing the log likelihood function

$$\ln L(\theta) = \sum_{S<t_i<T} \ln \lambda_\theta(t_i) - \int_S^T \lambda_\theta(t)\, dt \qquad (4)$$

(e.g. Daley and Vere-Jones, 2002). See Utsu and Ogata (1997) for the computational codes, especially associated with useful manuals for technical aspects in the fitting. Thus, we use the maximum likelihood estimate (MLE) $\hat{\theta}$ to predict the future occurrence rate $\lambda_{\hat{\theta}}(t)$. The period for which the ETAS model parameters are computed is called the target interval. In the figures of this paper, this is specifically denoted by (*Ts*, *Te*) or (*Ts*, *Tc*) in place of (*S*, *T*) in (4). The seismicity in this period may be affected by earthquakes that occurred before this period, due to the long-lived nature of aftershock activity. To consider this effect, a time interval precursory to the target interval (called precursory interval) is chosen and aftershock activities following earthquakes in this period are included in the computation. This is extremely important in the analysis of the aftershocks to

maintain the homogeneity or the completeness of the data, where the target period should exclude a short period immediately after the mainshock, due to the substantial exclusion of smaller aftershocks, whereas the mainshock and the large aftershocks are highly effective as the history to the future of the aftershock activity (e.g., see Ogata, 2001). When the ETAS parameters are estimated for two or more successive periods (usually divided at turning points *Tc* of seismicity), it is better to set a precursory period before each target period.

References

Abe, K., 1977. Tectonic implications of the large Shioya-Oki earthquakes of 1938, Tectonophysics, 41, 269-289.

Aida, I., 1977. Simulations of large tsunamis occurring in the past off the coast of Sanriku district (in Japanese), *Bull. Earthq. Res. Inst.*, **52**, 71-101.

Daley, D.J., Vere-Jones, D., 2002. *An Introduction to the Theory of Point Processes, Volume 1*, 2nd edition, Springer-Verlag, New York, 2002.

Dieterich, J., 1994. A constitutive law for rate of earthquake production and its application to earthquake clustering. *J. Geophys. Res.*, **99**, 2601–2618.

Geographical Survey Institute of Japan, 2004. Crustal movement in the Tohoku District, *Report of the Coordinating Committee for Earthquake Prediction*, **71**, 52.

Guo, Z., Ogata, Y., 1993. Statistical relations between the parameters of aftershocks in time, space and magnitude. *J. Geophys. Res.* **102**, 2857-2873.

Harris, R. A., 1998, Introduction to special section: Stress triggers, stress shadows, and implications for seismic hazard, *J. Geophys. Res.*, *103*, 24,347–24,358.

Headquarter for Earthquake Research Promotion of Japan, 2005. Updating of probabilities of the long-term earthquake forecasts and sizes of earthquakes based on the active fault data (in Japanese), http://www.jishin.go.jp/main/chousa/05jan_kakuritsu/p04_kaikou.pdf.

Ichikawa, M., 1971. Reanalyses of mechanism of earthquakes which occurred in and near Japan, and statistical studies on the nodal plane solutions obtained, 1926-1968, *Geophys. Mag.* (Tokyo), *35*, 207-274.

Inouye, W., 1965., On the seismicity in the epicentral region and its neighborhood before the Niigata earthquake (in Japanese), *Kenshin-jiho* (*Q. J. Seismol.*), 29, 139-144.

Japan Meteorological Agency, 2004. Mechanism data file, *The Annual Seismological Bulletin of Japan*.

Kanamori, H., 1972. Relation between tectonic stress, great earthquakes, and earthquake swarms, Tectonophysics, **4**, 1-12.

Kikuchi, M., Yamanaka, Y., 2003. EIC Seismological Note, Earthquake Research Institute, University of Tokyo, http://www.eri.u-tokyo.ac.jp/sanchu/Seismo_Note/index-e.html, No. 0, 50, 128, 135, 137

King, G.C.P., Stein, R., Lin, J., 1994. Static stress changes and the triggering of earthquakes. *Bull. Seismol. Soc. Am.*, **84**, 935-953.

Kisslinger, C., 1988. An experiment in earthquake prediction and the 7th May 1986 Andreanof *Islands* Earthquake. *Bull. Seismol. Soc. Am.*, **78**, 218-229.

Naito, H. and Yoshikawa, S., 1996. A program to assist crustal deformation analysis (in Japanese). *Zisin ii (J. Seismol. Soc. Japan)* 52, 101-103.

Lin, J., Stein, R.S., 2004. Stress triggering in thrust and subduction earthquakes, and stress interaction between the southern San Andreas and nearby thrust and strike-slip faults, *Journal of Geophysical Research,* 109, B02303, doi:10.1029/2003JB002607

Matsu'ura, R.S., 1986. Precursory quiescence and recovery of aftershock activities before some large aftershocks, *Bull. Earthquake Res. Inst. Univ. Tokyo*, *61*, 1–65.

Ohtake, M., Matumoto, T., Latham, G.V., 1977. Seismicity gap near Oaxaca, southern Mexico as a *probable* precursor to a large earthquake. *Pure Apple. Geophys.*, **115**, 375-385.

Ogata, Y., 1983. Estimation of the parameters in the modified Omori formula for aftershock frequencies by the maximum likelihood procedure, *J. Phys. Earth* **31**, 115-124.

Ogata, Y., 1988. Statistical models for earthquake occurrences and residual analysis for point processes. *J. Amer. Statist. Assoc.* **83**, 9-27.

Ogata, Y., 1992. Detection of precursory relative quiescence before great earthquakes through a statistical model, *J. Geophys. Res*., 97, 19,845–19,871.

Ogata, Y. 1999. Seismicity analyses through point-process modeling: A review, *Pure Appl. Geophys.*, 155, 471–507.

Ogata, Y., 2001. Increased probability of large earthquakes near aftershock regions with relative quiescence, *J. Geophys. Res.*, 106, 8729–8744.

Ogata, Y., 2004a. Space-time model for regional seismicity and detection of crustal stress changes. *J. Geophys. Res.*, **109,** 10.1029/2003JB002621.

Ogata, Y., 2004b. Seismicity quiescence and activation in western Japan associated with the 1944 and 1946 great earthquakes near the Nankai trough. *J. Geophys. Res.*, **109**, 10.1029/2003JB002634.

Ogata, Y., 2004c. Statistical Analysis of seismic activities in and around Tohoku District, northern Japan, prior to the large interpolate earthquakes off the coast of Miyagi Prefecture (in Japanese), *Report of the Coordinating Committee for Earthquake Prediction*, **71**, 268-278.

Ogata, Y., 2004d. Static triggering and statistical modelling (in Japanese), *Report of the Coordinating Committee for Earthquake Prediction*, **72**, 631-637.

Ogata, Y., 2005. Detection of anomalous seismicity as a stress change sensor, *J. Geophys. Res*., Vol. 110, No. B5, B05S06, 10.1029/2004JB003245.

Ogata, Y., Shimazaki, K., 1984. Transition from aftershock to normal activity: The 1965 Rat Islands earthquake aftershock sequence, *Bull. Seismol. Soc. Am.*, *74*, 1757–1765.

Ogata, Y., Jones, L. M., Toda, S., 2003. When and where the aftershock activity was depressed: Contrasting decay patterns of the proximate large earthquakes in southern California, *J. Geophys. Res.*, *108*(B6), 2318, doi:10.1029/2002JB002009.

Okada, Y., 1992. Internal deformation due to shear and tensile faults in a half-space. *Bull. Seism. Soc. Am*. 82, 1018-1040.

Omori, F., 1894. On the aftershocks of earthquakes, *J. Coll. Sci. Imp. Univ. Tokyo* **7**, 111-200.

Reasenberg, P., Jones, L.M., 1989. Earthquake hazard after a mainshock in California, *Science*, *243*, 1173–1176.

Reasenberg, P.A., Simpson, R.W., 1992. Response of regional seismicity to the static stress change produced by the Loma Prieta earthquake. *Science*, **255**, 1687-1690.

Research group for active faults in Japan, 1992. *Maps of Active Faults in Japan with an Explanatory Text*, University of Tokyo Press,

Seno, T., 1979. On the earthquake expected off the Miyagi prefecture (in Japanese), *Report of the Coordinating Committee for Earthquake Prediction*, **21**, 38-43.

Seno, T., K. Sudo, Eguchi, T., 1979a. Focal mechanism of the Miyagi-Ken-Oki earthquake of June 12, 1978 (in Japanese), *Report of the Coordinating Committee for Earthquake Prediction*, **21**, 10-12.

Stein, R.S., 1999. The role of stress transfer in earthquake occurrence, *Nature*. **402**, 605-609.

Toda, S., Stein, R.S., Reasenberg, P., Dieterich, J.H., Yoshida, A., 1998. Stress transferred by the M_w = 6.9 Kobe, Japan, shock: Effect on aftershocks and future earthquake probabilities, *J. Geophys. Res.*, 103, , 24543-24545.

Toda, S. and R.S. Stein, 2002. Response of the San Andreas Fault to the 1983 Coalinga-Nuñez Earthquakes: An Application of Interaction-based Probabilities for Parkfield. *J. Geophys. Res.* **107**, 10.1029/2001JB000172.

Tohoku University, 1995. Faulting process of the 1994 Far East Off Sanriku earthquake inferred from GPS observation. *Report of the Coordinating Committee for Earthquake Prediction*, **54,** 97-101.

Tsuruoka, H., 1996. Development of seismicity analysis software on workstation (in Japanese). *Tech. Res. Rep*. **2** 34-42, Earthquake Res. Inst., Univ. Tokyo.

Uchida, N., Matsuzawa, T., Igarashi T., Hasegawa, A., 2003. Interplate quasi-static slip off Sanriku, NE Japan, estimated from repeating earthquakes, *Geophys. Res. Lett*., 30, 10.1029/2003GL017452.

Uchida, N., Hasegawa, A., Matsuzawa, T., Igarashi, T., 2004. Pre- and post-seismic slow slip on the plate boundary off Sanriku, NE Japan associated with three interplate earthquakes as estimated from small repeating earthquake data, *Tectonophysics*, 385, 1-15.

Utsu, T., 1961. A statistical study on the occurrence of aftershocks, *Geophys. Mag.* **30**, 521-605.

Utsu, T., 1968. Seismic activity in Hokkaido and its vicinity (in Japanese). *Geophys. Bull. Hokkaido Univ.*, **13**, 99-103.

Utsu, T., 1969, Aftershocks and earthquake statistics (I): some parameters which characterize an aftershock sequence and their interaction, *J. Faculty Sci., Hokkaido Univ., Ser. VII*, 3, 129-195.

Utsu, T., 1970. Aftershocks and earthquake statistics (II): Further investigation of aftershocks and other earthquakes sequence based on a new classification of earthquake sequences, *J. Faculty Sci., Hokkaido Univ., Ser. VII* **3**, 379-441.

Utsu, T., 1984. Estimation of parameters for reccurrence models of earthquakes, *Bull. Earthq. Res. Inst.*, **59**, 53-66.

Utsu, T., Ogata, Y., Matsu'ura, R. S., 1995, The centenary of the Omori formula for a decay law of aftershock activity, *J. Phys. Earth*, *43*, 1–33.

Utsu, T., Ogata, Y., 1997. Statistical Analysis of point processes for Seismicity (SASeis). *IASPEI Software Library* **6**, 13-94, International Association of Seismology and Physics of Earth's Interior.

Wyss, M., Burford, R.O., 1987. A predicted earthquake on the San Andreas fault, California. *Nature* **329,** 323-325.

Yamanaka, Y., Kikuchi, M., 2001. Asperity map based on the analysis of historical seismograms: Tohoku version, Abstracts of the 2001 Joint Meeting for Earth and Planetary Science, Sy-005.

Yamanaka Y., Kikuchi, M., 2004. Asperity map along the subduction zone in northeastern Japan inferred from regional seismic data, *J. Geophys. Res.*, 109, B07307, doi:10.1029/2003JB002683.

Table 1. Assumed source fault parameters of the Miyagi-Ken-Oki earthquakes

Year	M	Long.	Lat.	Dep (km)	Strike (deg)	Dip (deg)	Rake (deg)	L (km)	W (km)	Slip (cm)	References
1793	8.2	143.58	39.16	1	205	40	90	120.	30.	390.	Aida (1977)
1936	7.4	142.7	38.3	15	190	20	90	80.	60.	200.	Seno et al. (1979)
1978	7.4	142.43	38.42	25	190	20	76	30.	80.	170.	Seno et al. (1979)
2003	7.0	141.81	38.94	52	192	68	73	17.	19.	210	G. S. I. J. (2003)

Table 2. Assumed receiver fault angles and Δ*CFS* values

Regions	Strike (deg.)	Dip (deg.)	Rake (deg.)	Depth (km)	Δ*CFS* [*1] (milli-bars)	Seismicity
Fig. 1	200	45	90	20	**-5. ~ -1.**	**Quiet**
Fig. 2A	180	45	270	20	**-3. ~ -1.**	**Quiet**
Fig. 2B	200	20	90	-- [*2]	**+50. ~ +200.**	**Normal**
Fig. 3	200	45	90	20	**-10. ~ -5.**	**Quiet**
Fig. 4	190	30	76	-- [*2]	**-0.05 ~ +0.4**	**Normal**
Fig. 5	194	74	85	50	**-100.**	**Quiet**

(*1) 10% of the slip-size of the rupture model in Table 1 is assumed for the precursory slip. The depth in (*2) is on descending interface between the inland plate and subducting slub. The bold face numbers indicate the consistency of the Δ*CFS* signs with the analyzed result of the seismic activity.

Table 3. Assumed receiver fault angles and Δ*CFS* values

Receiver regions	Angles[*1]			dep km	Δ*CFS* [*2] (millibars)				Seismicity
	θ	δ	λ		1973	1936	1978	**2003**	
Fig. 6	10	30	90	20	-3 ~ -2	-10 ~ -1	-3 ~ -1	**+.3~ +2**	**Normal**
Fig. 7	190	30	76	--[*4]	**+5~ +8**	**+.5~ +2**	**+.5~ +1**	**+.1~ +.5**	**Normal**
Fig. 8	192	68	73	52	**+10**	**+50**	**+7**	**---**	**Normal**
Fig. 9	201	42	102	10	-20	**-/+** [*5]	-50	**+10** [*3]	**Normal**
Fig. 10A	211	41	128	10	-20	-10	-20	**+5**	**Normal**
Fig. 10B	199	45	105	10	-20	-20	-10	**+4**	**Normal**
Fig. 10C	187	37	52	10	-/+	+5	**-30**	**-1**	**Quiet**
Fig. 10D	216	41	131	10	-8	**+2**	**+1**	**+.5**	**Normal**
Fig. 10E	181	22	70	46	+80	+50	+20	**-20**	**Quiet**

(*1) θ, δ and λ represents strike, dip and rake angles in degrees, respectively. (*2) 10% of the slip-size of the rupture model in Table 1 is assumed for the precursory slip except for (*3) that is coseismic. The depth in (*4) is along descending interface between the inland plate and subducting slub. (*5) -/+ means neutral. The bold face numbers indicate the consistency of the signs with the analyzed result of the seismic activity.

Figure Captions:

Fig.1. Shallow earthquakes (M≥4) in the stress-shadow region during the period 1926–1937, before and after the 1936 Miyagi-Ken-Oki earthquake of M7.4: (a) epicenters, (b) longitude versus time, and (c) cumulative numbers and magnitude against time. The gray color shows the stress-shadow region of thrust-type faults under EW-compression (cf., Table 2) at a 10km depth, assuming the preslip within or around the 1936 rupture fault. The vertical dotted line indicates the 1936 event.

Fig.2. Aftershocks of the 1933 Sanriku-Oki earthquake of M8.1 (Region A ; M≥4.3), and seismic activity before 1938 great swarm at Shioya-Oki (Region B; M≥4.2): (a) epicenters and the 1936 source model, (b) and (c) cumulative numbers and magnitude against the ordinary time (top panel) and transformed time (bottom panel) for the regions A and B, respectively. Hereafter, vertical dotted lines denoted by *Ts*, *Te*, and *Tc* show that ETAS is fitted to the events in the target periods of either (*Ts*, *Te*) or (*Ts*, *Tc*) where the time *Tc* is the turning point to the quiescence. In the cases of (b) and (c), the time *Ts* is 0.15 day after the mainshock and beginning of 1926, respectively, and the time *Te* for both cases is the end of 1938. The vertical line at *Tc* in (c) indicates the occurrence of the 1936 rupture.

Fig.3. Shallow earthquakes (M≥4) during the period 1964-1980, including the aftershocks of the 1964 Niigata earthquake of M7.5 in the stress-shadow region, before and after the 1978 Miyagi-Ken-Oki earthquake of M7.4: (a) epicenters, the 1978 source model, and longitude versus time, and (b) cumulative numbers and magnitude against the ordinary and transformed times. The gray color in the epicenter plots shows stress-shadow region at a 10km depth, assuming the preslip within or around the 1978 rupture fault. The quiescence after 1975 (dotted vertical line at *Tc*) is seen in the stress-shadow region, where the ΔCFS ranges - 5 ~ - 10 millibars transferred from the assumed preslip of the 1978 rupture.

Fig.4. Aftershocks (M≥5) of the 1968 Tokachi-Oki earthquake of M7.9. (a) epicenters and the 1978 source model, and (b) cumulative numbers and magnitude against the ordinary and transformed times. In this case, *Ts* is 0.2 days after the mainshock and *Te* is the occurrence time of the 1978 Miyagi-Ken-Oki event. We see no seismicity changes, even after the 1978 rupture.

Fig.5. Panels show that the aftershocks (M≥4) of the Ojika-Hanto-Oki earthquake of M6.7 occurred on 20 February, 1978. We see the relative quiescence one and a half months after the

mainshock up until the main rupture of M7.4 on 12 June, 1978.

Fig.6. Shallow earthquakes ($M \geq 4$) including the aftershocks of the 1983 Central Sea of Japan earthquake of M7.7 in the stress-shadow (gray color) region during 1978 - 20 July, 2003, assuming the preslips of the interplate rupture (cf., Table 1), (a) epicenters and (b) cumulative numbers and magnitude against the ordinary and transformed times. (*Ts, Te*) in this case covers the entire period of the data.

Fig.7. The aftershocks ($M \geq 3.5$) of the 1994 Sanriku-Haruka-Oki earthquake of M7.5 and background activity in and around the region. In this case, the time *Ts* is 10 days after the mainshock (i.e., after the largest aftershock of M7.2) and the time *Te* is 20 July, 2003.

Fig.8. Aftershock sequences ($M \geq 1.5$) of the 2003 Miyagi-Ken-Oki earthquake of M7.0, which has a similar mechanism to that of the Ojika-Hanto-Oki earthquake, where *Ts* = 0.1 days after the mainshock.

Fig.9 Aftershock sequences ($M \geq 1.5$) of the 2003 Northern Miyagi-Ken earthquake of M6.3, where *Ts* = 0.05days after the mainshock.

Fig.10. Recent aftershock or swarm activity of (A) the 1962 Miyagi-Ken-Hokubu earthquake of M6.5, (B) the 1996 Miyagi-Ken Naruko-Machi earthquake of M5.9, (C) the 1998 Miyagi-Ken-Nanbu earthquake of M5.0, (D) the 1998 Iwate-Ken Shizukuishi earthquake of M6.1, and (E) the 2002 Miyagi-Ken-Oki earthquake of M6.1. The values of *Ts*, *Tc* and *Te* are indicated in the panel.

Figure 1.

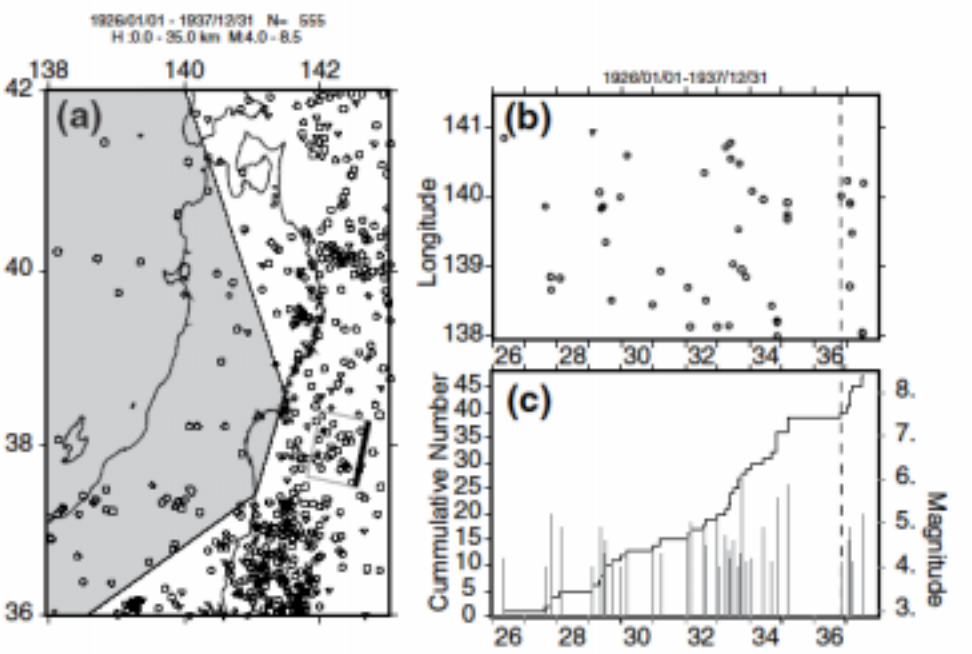

Figure 2.

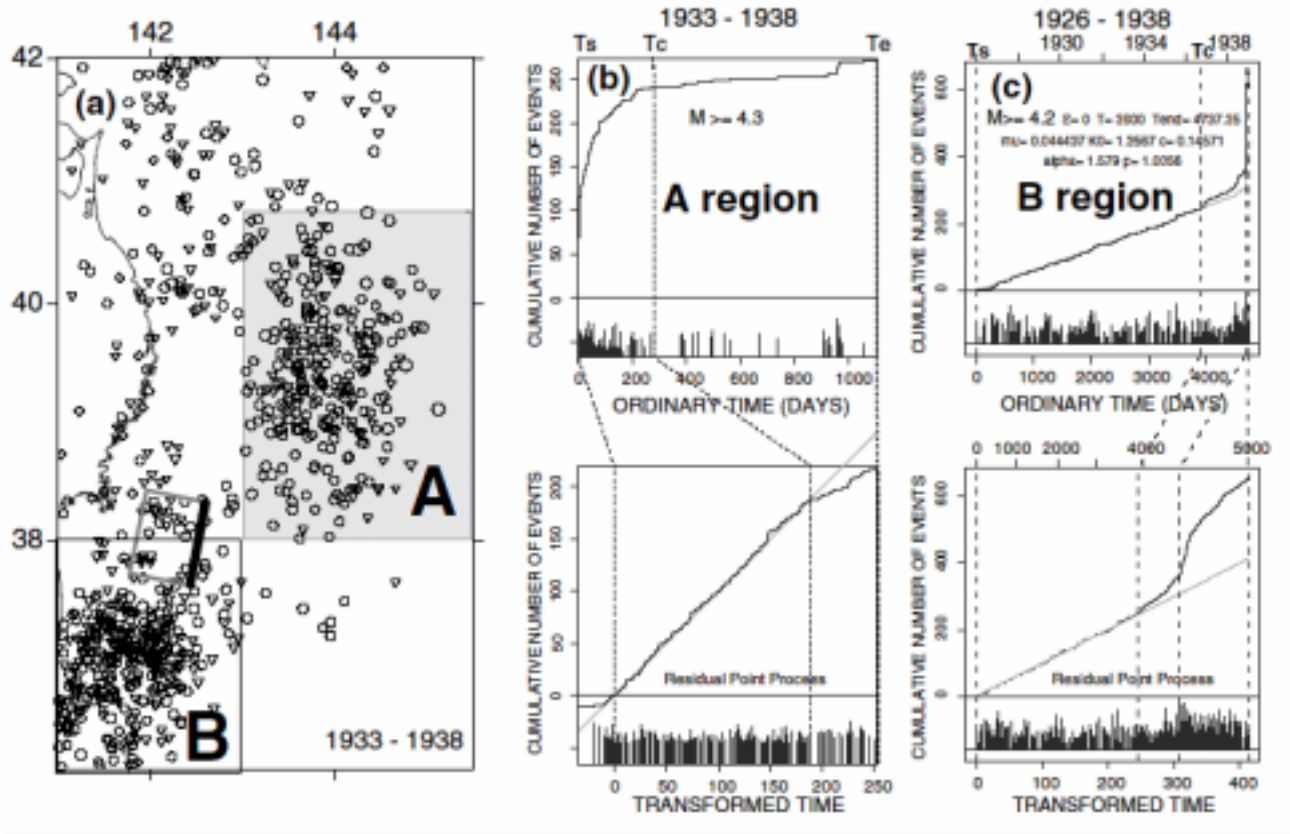

Figure 3.

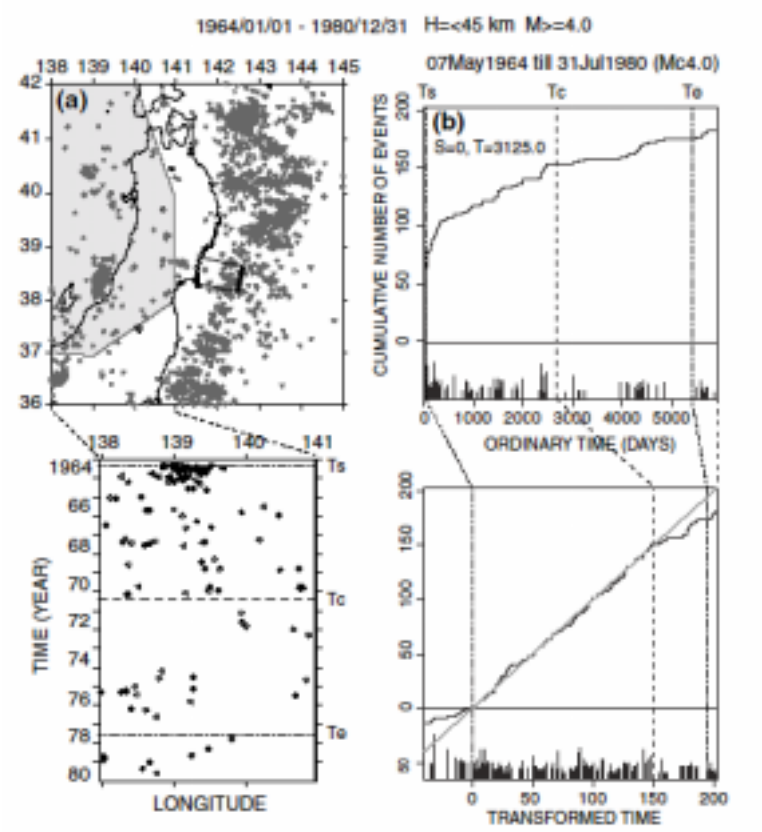

Fugure 4.

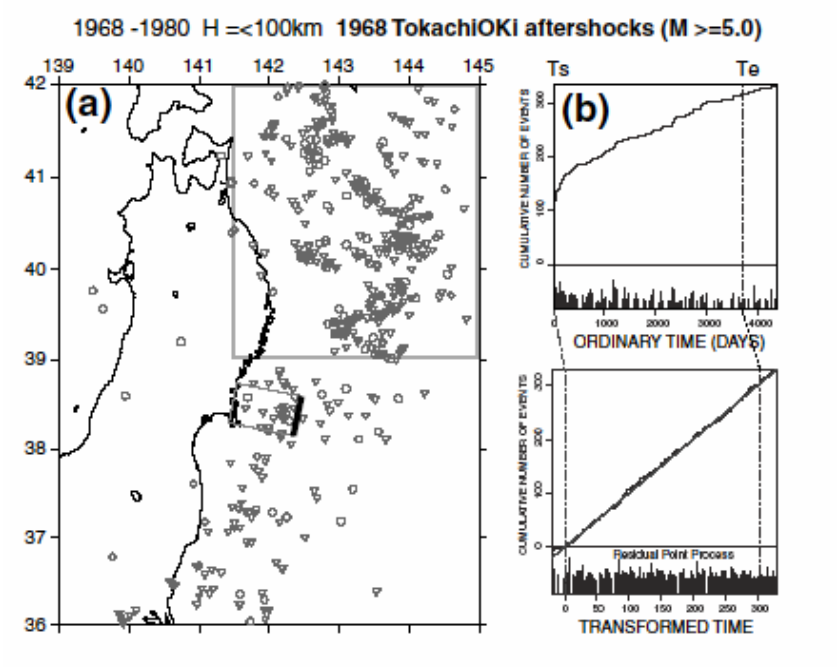

Figure 5.

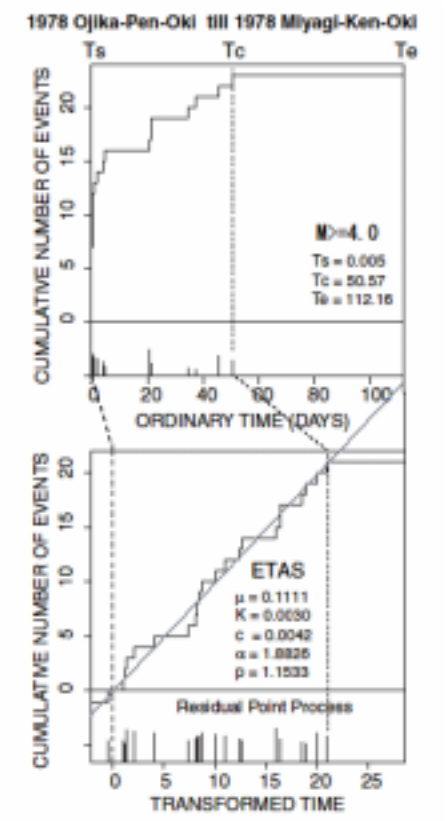

Figure6.

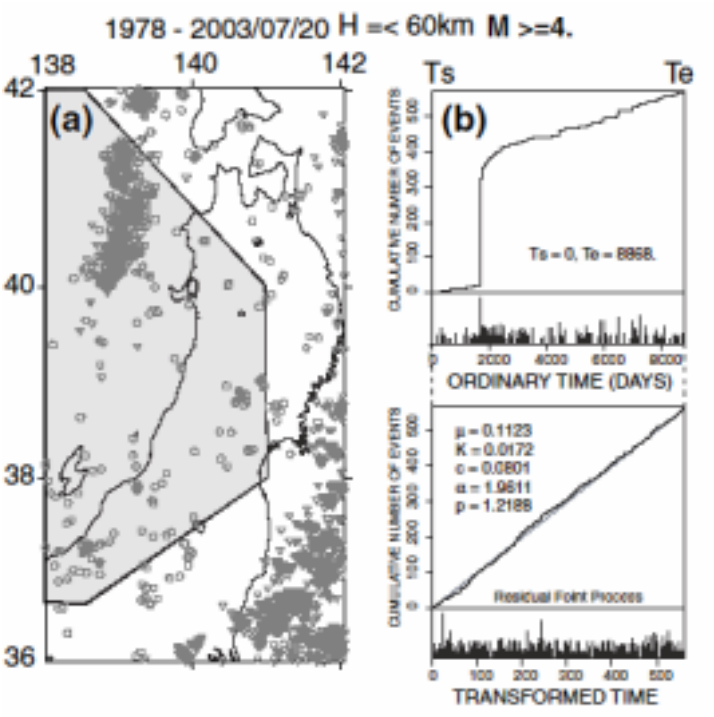

Figure 7.

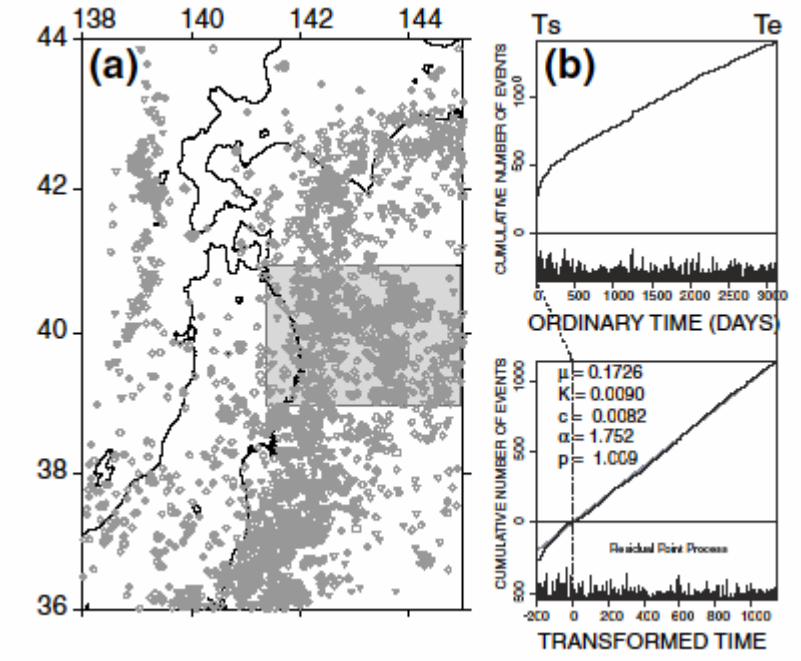

Figure 8.

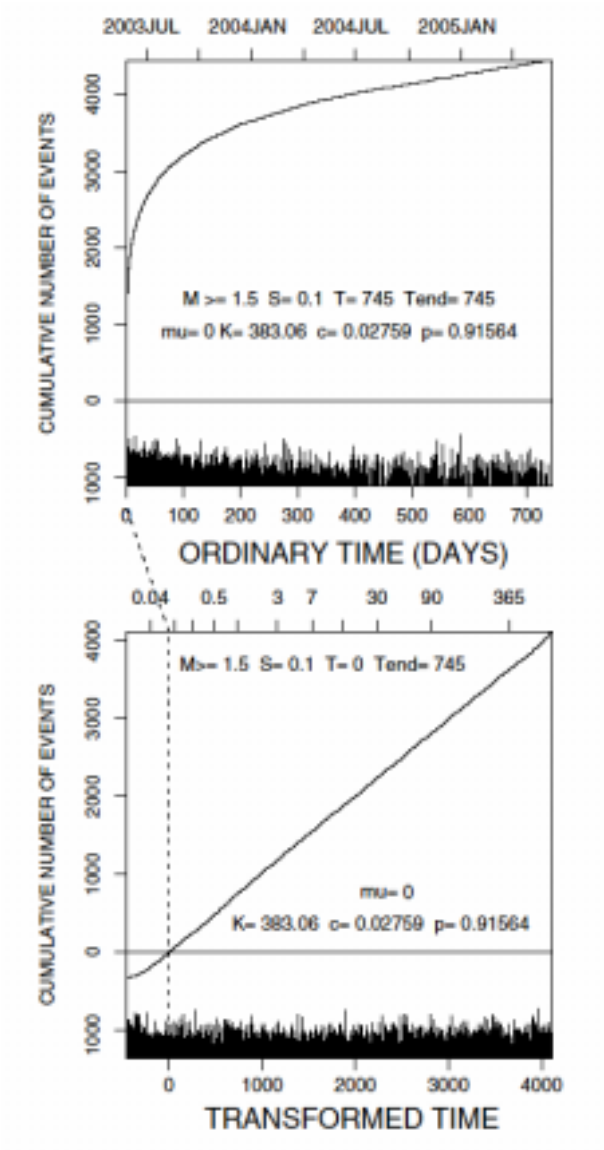

Figure 9.

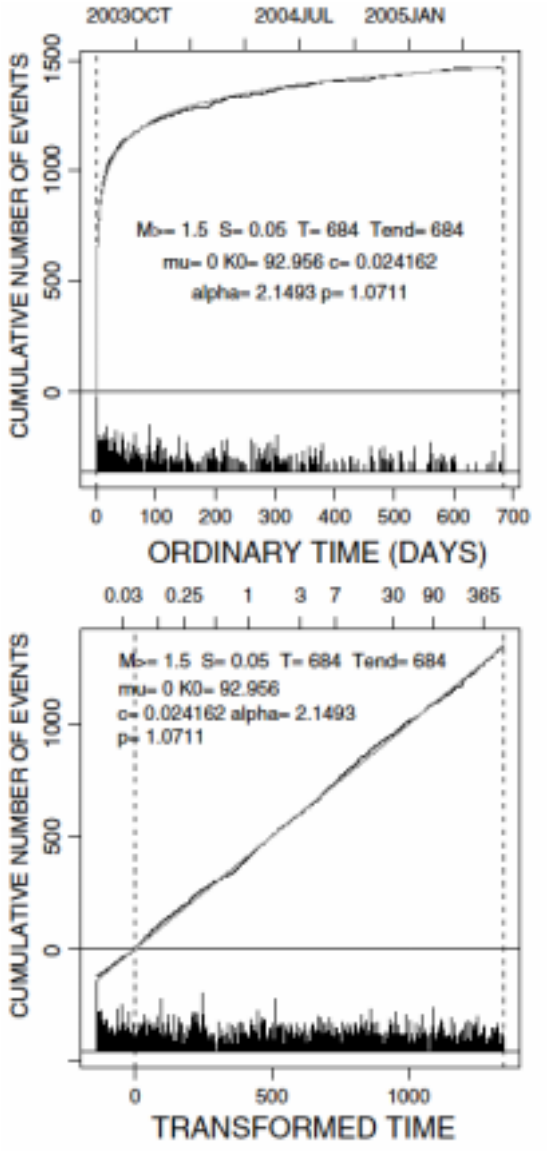

Figure 10.

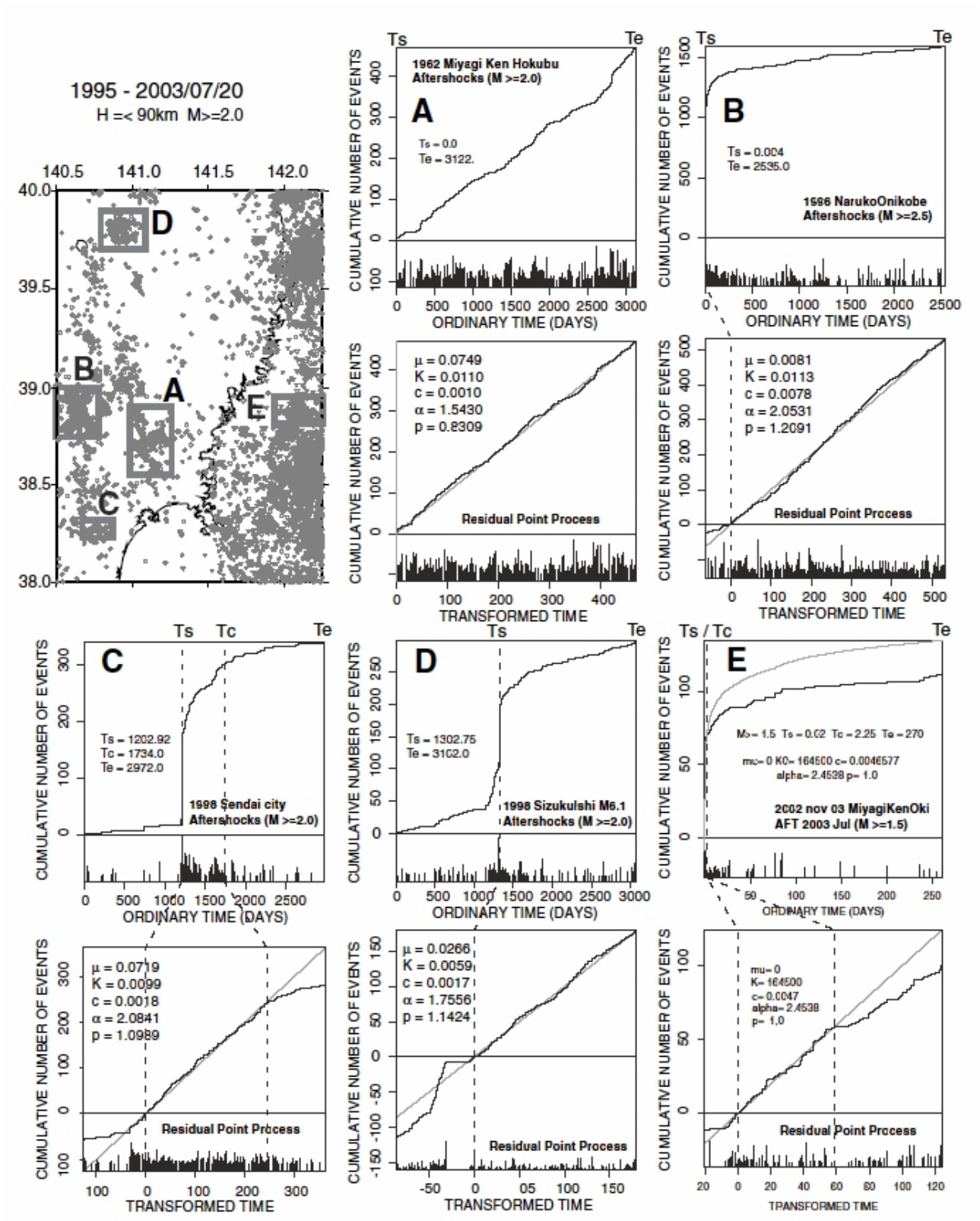
1995 - 2003/07/20
H =< 90km M>=2.0
140.5
141.0
141.5
142.0
40.0
39.5
39.0
38.5
38.0
A
B
C
D
E
Ts
Te
1962 Miyagi Ken Hokubu
Aftershocks (M >=2.0)
Ts = 0.0
Te = 3122.
CUMULATIVE NUMBER OF EVENTS
ORDINARY TIME (DAYS)
μ = 0.0749
K = 0.0110
c = 0.0010
α = 1.5430
p = 0.8309
Residual Point Process
TRANSFORMED TIME
Ts
Te
B
Ts = 0.004
Te = 2535.0
1996 NarukoOnikobe
Aftershocks (M >=2.5)
ORDINARY TIME (DAYS)
μ = 0.0081
K = 0.0113
c = 0.0078
α = 2.0531
p = 1.2091
Residual Point Process
TRANSFORMED TIME
Ts
Tc
Te
C
Ts = 1202.92
Tc = 1734.0
Te = 2972.0
1998 Sendai city
Aftershocks (M >=2.0)
ORDINARY TIME (DAYS)
μ = 0.0719
K = 0.0099
c = 0.0018
α = 2.0841
p = 1.0989
Residual Point Process
TRANSFORMED TIME
Ts
Te
D
Ts = 1302.75
Te = 3102.0
1998 Sizukuishi M6.1
Aftershocks (M >=2.0)
ORDINARY TIME (DAYS)
μ = 0.0266
K = 0.0059
c = 0.0017
α = 1.7556
p = 1.1424
Residual Point Process
TRANSFORMED TIME
Ts / Tc
Te
E
M>= 1.5 Ts = 0.02 Tc = 2.25 Te = 270
mu= 0 K0= 164500 c= 0.0046577
alpha= 2.4538 p= 1.0
2002 nov 03 MiyagiKenOki
AFT 2003 Jul (M >=1.5)
ORDINARY TIME (DAYS)
mu= 0
K= 164500
c= 0.0047
alpha= 2.4538
p= 1.0
Residual Point Process
TPANSFORMED TIME